iScience

CellPress
OPEN ACCESS

Article

# PVA/PAA/DMTD electrospun nanofibrous membrane for the selective adsorption of Pb(II) ions in liquid foods

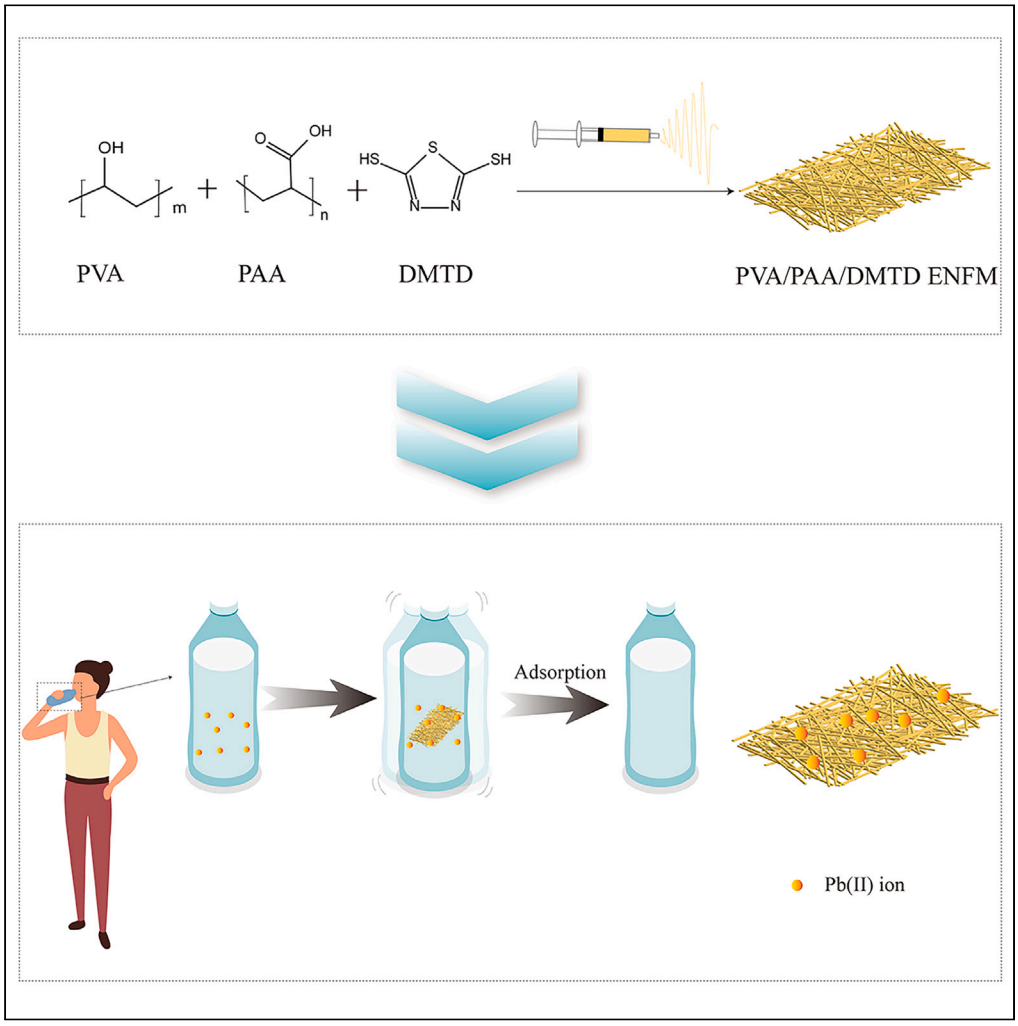


Han Wang, Dongtian Miao, Yongjiang Yu, Zhihan Zhang, Youlong Zhu, Qing Wang

zhuyl9@mail.sysu.edu.cn (Y.Z.)
wangq27@mail.sysu.edu.cn (Q.W.)

## Highlights

The PVA/PAA/DMTD ENFM was invented for the selective adsorption of Pb(II) ions

The PVA/PAA/DMTD ENFM exhibited high efficiency for Pb(II) ions removal in liquids

The PVA/PAA/DMTD ENFM showed good selectivity and reusability for Pb(II) removal

Wang et al., iScience 27, 108737
January 19, 2024 
https://doi.org/10.1016/j.isci.2023.108737

iScience

CellPress
OPEN ACCESS

Article

# PVA/PAA/DMTD electrospun nanofibrous membrane for the selective adsorption of Pb(II) ions in liquid foods

Han Wang,[1,3] Dongtian Miao,[2,3] Yongjiang Yu,[1] Zhihan Zhang,[1] Youlong Zhu,[2,*] and Qing Wang[1,4,*]

## SUMMARY

**Lead (Pb(II)) contamination is common in liquid foods and can result from Pb(II) being present in the raw materials or during handling processes. However, due to the complexity of food matrices, there is limited data available concerning Pb(II) ion removal from food sources. This study focused on fabricating a PVA/PAA/DMTD electrospun nanofibrous membrane (ENFM) to efficiently and selectively remove Pb(II) ions from liquid foods. The PVA/PAA/DMTD ENFM had a maximum adsorption capacity of 138.3 mg/g for Pb(II) ions and demonstrated high selectivity toward the removal of Pb(II) ions. Negative values of the Gibbs free energy ($\Delta G^{\circ}$) showed that the spontaneous nature of the adsorption process was feasible at different temperatures. Moreover, it successfully removed Pb(II) ions from selected samples of commercially available drinks. Therefore, this adsorbent exhibits significant potential for removing Pb(II) ions from liquid food products, thereby reducing daily dietary exposure to Pb(II).**

## INTRODUCTION

Lead (Pb(II)) is a heavy metal that is broadly employed in various industrial processes, and particularly in the manufacturing of pipes, paints, and pigments, due to its corrosion resistance. The discharge of industrial wastewater leads to environmental water resources and soil pollution. Beverages are prone to Pb(II) contamination due to the presence of Pb(II) in raw materials or exposure to lead-containing materials during packaging, storage, and other handling processes.[1,2] Recently, there has been evidence that the popularity of non-alcoholic beverages among children and adolescents is increasing.[3,4] Additionally, studies have demonstrated that food constitutes a significant source of Pb(II) exposure for children.[5] Even low levels of Pb can pose serious health hazards to children, including anemia, decreased immunity, memory loss, and cardiovascular stress.[6,7] Currently, Pb(II) content in liquid foods exceeding the national food safety standard remains an occasional occurrence in certain developing countries.[8–10] For example, Sylvester et al. discovered that the Pb(II) content in multiple non-alcoholic beverages in Nigeria exceeded the limits established by both the World Health Organization (WHO) and Nigerian standards.[9]

Consequently, numerous technologies have been developed to address the removal of Pb(II) ions from liquid foods with the aim of mitigating the population's exposure to Pb(II). These technologies encompass ion complexation, exchange, and adsorption.[11,12] Currently, the adsorption technique is widely recognized as one of the most efficacious means of removing Pb(II) ions from liquid food due to its advantages of high efficiency, ease of operation, and lack of secondary pollution.[13,14] However, most powder-based adsorbents, such as chitosan,[15] activated carbon,[16] and zeolite,[17] have drawbacks including poor selectivity, difficulty in separation and recovery, and unsuitability for removing low-concentration Pb(II) ions.[18]

Electrospinning offers a straightforward approach for fabricating fibers with diameters that cover the range from nanometers to submicron.[19,20] Electrospun nanofibrous membranes (ENFMs), known for their ample porosity, substantial specific surface area, ease of modification, and convenient separation and recovery, are highly suitable for adsorbing pollutants in water treatment and have attracted considerable interest among researchers.[21,22] In the electrospinning process, a polymer solution is ejected from the tip of a needle as an electric field is applied. The charged liquid jet is pushed toward the collector, a process in which the solvent undergoes evaporation, leading to the solidification of the polymer into nonwoven fibrous nanofibers deposited on the collector.[23]

In a previous study, poly(vinyl) alcohol/poly(acrylic) acid (PVA/PAA) fibers were successfully fabricated by employing the electrospinning technique, providing adsorption sites for metal cations by virtue of the existence of carboxyl and hydroxyl groups.[24] Heat treatment can improve the water resistance of PVA without the use of toxic cross-linkers.[25] In fact, the liquid food environment necessitates adsorption materials with enhanced selectivity to eliminate Pb(II) ions from liquid foods. From the application perspective, it is important to study the selectivity of adsorption because other metal ions in liquid foods may interfere with the adsorption process. Additionally, it is undesirable for the

[1]Department of Toxicology, School of Public Health, Guangdong Provincial Key Laboratory of Food, Nutrition and Health, Sun Yat-sen University, Guangzhou 510080, China
[2]PCFM Lab, School of Chemistry, Sun Yat-sen University, Guangzhou 510006, China
[3]These authors contributed equally
[4]Lead contact
*Correspondence: zhuyl9@mail.sysu.edu.cn (Y.Z.), wangq27@mail.sysu.edu.cn (Q.W.)
https://doi.org/10.1016/j.isci.2023.108737

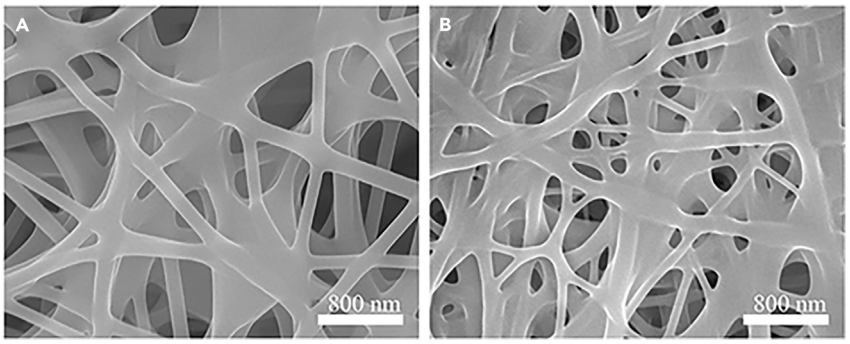


**Figure 1. Fiber structure of ENFMs**
SEM images of the (A) PVA/PAA ENFM and (B) PVA/PAA/DMTD ENFM.

adsorbent to remove Pb(II) ions that would substantially reduce certain metal elements in foodstuffs that are beneficial to human nutrition. 2,5-Dimercapto-1,3,4-thiadiazole (DMTD) contains abundant sulfur (S) and nitrogen (N) elements and possesses a highly conjugated structure, enabling excellent coordination and responsiveness to Pb(II) ions.[26–29] Thus, DMTD is an ideal additive for enhancing the selectivity of the PVA/PAA nanofiber membrane for Pb(II) ions.

In this work, we prepared a PVA/PAA/DMTD ENFM by incorporating DMTD into the polymer solution to achieve the efficient and selective reduction of trace amounts of Pb(II) ions in various liquid foods. The performance of removing Pb(II) ions in aqueous solutions was then evaluated by conducting batch adsorption experiments. We also explored the effect of pH values on the removal of Pb(II) ions and evaluated the selectivity of the adsorbent to Pb(II) using various metal ions. Furthermore, the regeneration ability of the PVA/PAA/DMTD ENFM for the adsorption of Pb(II) ions was examined. Finally, we attempted to adsorb Pb(II) ions in commercially available liquid foods, and we obtained a satisfactory removal efficiency. Our study contributes to advancing the research direction of Pb(II) removal technologies in liquid foods.

## RESULTS AND DISCUSSION

### Characterization

The morphologies of the PVA/PAA ENFM and the PVA/PAA/DMTD ENFM were obtained from the SEM (Figure 1). The PVA/PAA ENFM exhibited fibers with consistent diameters (156.8 ± 39.6 nm), smooth fiber surfaces, and randomly distributed fiber networks. Importantly, the incorporation of DMTD led to a substantial reduction in the pore sizes of the ENFM.

The FT-IR spectra of PVA/PAA/DMTD ENFM, PVA/PAA ENFM, and DMTD monomer in the range of wavenumbers from 4,000 to 400 $cm^{-1}$ are illustrated in Figure 2A. The peaks detected at 1,091 and 1,237 $cm^{-1}$ corresponded to the stretching vibrations of C-O and C-C, respectively. The peak at 1,704 $cm^{-1}$ was attributed to the ester group (COO) of PAA/PVA.[24,30] For the DMTD monomers, the characteristic bands at 2,854 and 2,476 $cm^{-1}$ correspond to S-H stretching vibrations,[31] the bands at 1,501, 1,262, 1,119, 1,049, and 712 $cm^{-1}$ were classified as N-H in-plane deformation, the thioamide II mode, thiadiazole ring skeleton stretching, N-N stretching, and the C-S-C endocyclic asymmetric stretch,

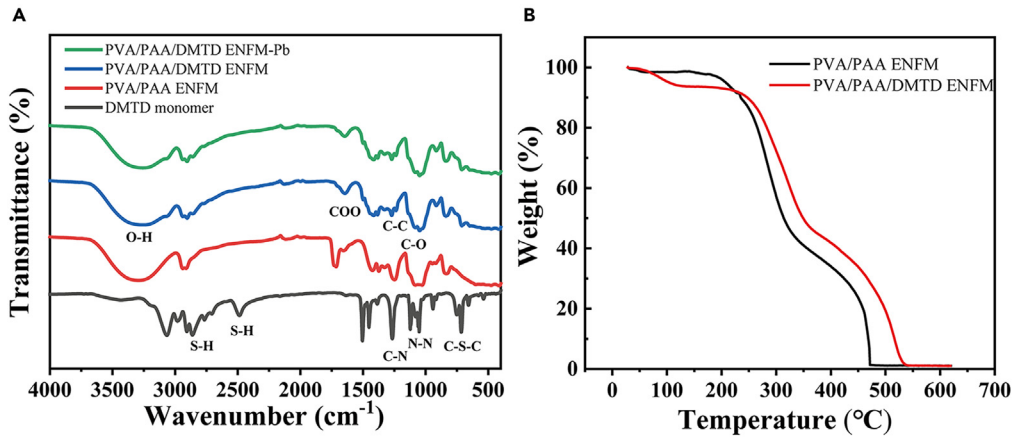


**Figure 2. Chemical structure and stability of ENFMs**
(A) The FT-IR spectra of the PVA/PAA/DMTD ENFM before and after adsorption of Pb(II), the PVA/PAA ENFM, and (B) the DMTD monomer, and the TGA curves of the PVA/PAA ENFM and PVA/PAA/DMTD ENFM.

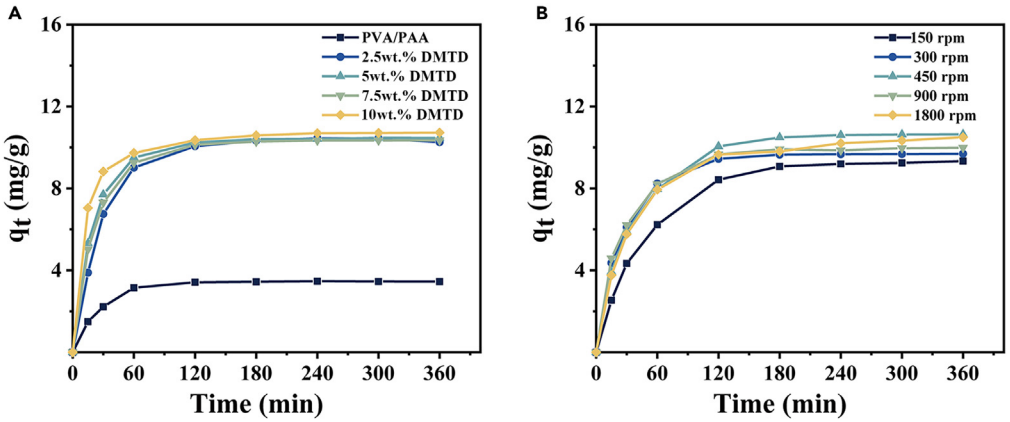


**Figure 3. Effect of preparation conditions**

The impact of (A) the DMTD concentration and (B) rotational speed of the PVA/PAA/DMTD ENFM on the adsorption capacity for Pb(II) ions. Data are represented as the mean values of the three groups.

respectively.[32] Consequently, the spectrum of the PVA/PAA/DMTD ENFM exhibited distinct characteristic peaks, confirming the successful incorporation of DMTD into the composite. Additionally, the FT-IR spectra showed that the PVA/PAA/DMTD ENFM had essentially identical characteristic peaks before and after the adsorption of Pb(II). This proved that the adsorbent had good stability during the adsorption process.

The thermogravimetric analysis (TGA) was used to obtain the thermal characteristics. Figure 2B shows the weight loss with increasing temperature for both samples (PVA/PAA ENFM and PVA/PAA/DMTD ENFM) via the TGA curves. The results of the thermogravimetric analysis of the PVA/PAA/DMTD ENFM were very similar to those of the PVA/PAA ENFM, both showing some water loss below 100°C and a thermal decomposition process that began near 200°C and continued until 500°C. The weight loss of the PVA/PAA ENFM and PVA/PAA/DMTD ENFM began from the temperature onsets of 183°C and 214°C, respectively, to nearly complete thermal degradation at 473°C and 537°C, respectively. This indicated that the addition of DMTD increased the thermal stability of the materials.

## Effect of the DMTD concentration and the rotational speed of the collector during preparation

The SEM images that are shown in Figure S1 illustrate the morphologies of the PVA/PAA ENFM and PVA/PAA/DMTD ENFM with varying mass concentrations of DMTD (2.5 wt.%, 5 wt.%, 7.5 wt.%, and 10 wt.%). The addition of DMTD led to a gradual unevenness in the diameter of the PVA/PAA/DMTD nanofibers. The effect of the DMTD content in the PVA/PAA/DMTD ENFM on the removal performance of Pb(II) ions was subsequently assayed in an aqueous solution of 1 mg/L Pb(II). We found that the adsorption capacity of the ENFM mixed with DMTD was 10.2–10.7 mg/g, which was much greater than that of the original PVA/PAA ENFM (3.4 mg/g) (Figure 3A). The influence of the DMTD addition on the adsorption performance was also explored. The adsorption capacity of the fiber membranes mixed with 5 wt.%, 7.5 wt.%, and 10 wt.% DMTD displayed a similar trend and all above 2.5 wt.%. Concurrently, the average pore size of the fiber membrane exhibited a decreasing trend with increasing DMTD content. However, further increases in the DMTD dosage beyond 7.5 wt.% resulted in damage to the fibrous membrane integrity. During the initial 2 h of adsorption, the ENFM doped with 5 wt.% DMTD demonstrated both a superior adsorption efficiency and a well-maintained fiber network integrity compared with those doped with 2.5, 7.5, and 10 wt.% DMTD. The PVA/PAA/DMTD ENFM was prepared using 5 wt.% DMTD for the subsequent experiments.

The rotational speed of the electrospinning device's mandrel (with a diameter of 8 cm) can influence the pore size of the fiber membrane, consequently impacting its adsorption performance.[33] The PVA/PAA/DMTD ENFM was prepared at speeds of 150, 300, 450, 900, and 1,800 rpm. The morphological structures of the PVA/PAA/DMTD ENFM were characterized by SEM. Figure S2 reveals a gradual decrease in the pore size with an increasing rotational speed. The adsorption efficacy of the PVA/PAA/DMTD ENFM with varying pore sizes was evaluated in an aqueous solution containing 1 mg/L Pb(II) ions. As depicted in Figure 3B, the PVA/PAA/DMTD ENFM collected at 150 rpm had a looser pore structure, resulting in the lowest adsorption efficacy for Pb(II) ions compared with the others. Its equilibrium adsorption capacity was only 9.2 mg/g. The adsorption performances of the other four groups were similar. Therefore, 450 rpm was chosen to ensure a rich pore structure and optimal adsorption capacity.

## Effect of the aqueous pH value, adsorption time, and initial concentration value on the Pb(II) adsorption

The solution's pH values were adjusted to 2 ± 0.1, 3 ± 0.1, 4 ± 0.1, 5 ± 0.1, 6 ± 0.1, 7 ± 0.1, and 8 ± 0.1 to determine the ideal pH level for the effective adsorption of Pb(II) ions. The Pb(II) ion removal efficiency increased with increasing pH values in the pH range of 2.0–5.0 (Figure 4). Additionally, the Pb(II) ion removal efficiency reached 95% at a pH value of approximately 5.0, with the adsorption capacity of the PVA/PAA/DMTD ENFM for Pb(II) reaching its maximum at approximately 12.14 mg/g. In a relatively acidic environment, the competitive $H^+$-Pb(II) interaction leads to a reduced adsorption efficiency for Pb(II) ions in a low-pH solution.[34] With a rise in the solution pH, electrostatic repulsion and competitive interactions gradually decreased as a result of the weakened ionization of Pb(II) and functional groups, resulting in an increase in

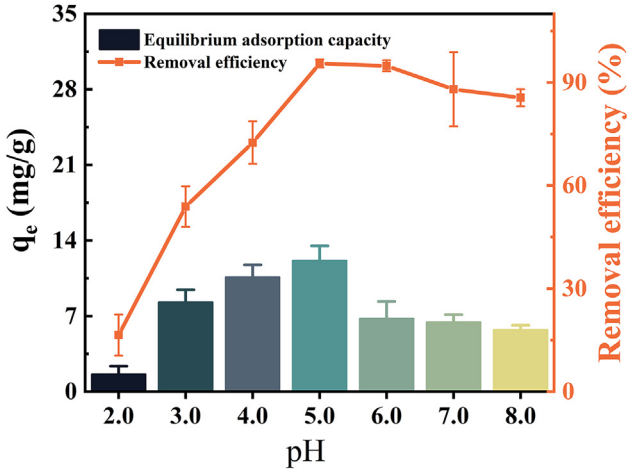


**Figure 4. The effect of the pH value of the solution on both the removal efficiency and the adsorption capacity of the PVA/PAA/DMTD ENFM for Pb(II) ions**

Data are represented as means ± SDs, n = 3.

the adsorption capacity.[35] Nevertheless, Pb(II) tends to precipitate at pH values exceeding 5.0,[24] resulting in a decreased efficiency in removing Pb(II) by the fibrous membranes. Subsequently, the removal of Pb(II) ions by the PVA/PAA/DMTD ENFM was investigated in the follow-up study, with the solution pH value controlled at 5.0.

To ensure that the adsorption process reached equilibrium and the adsorbent was fully utilized, the influence of the adsorption time on Pb(II) removal was tested. The initial Pb(II) ions content was controlled at 1 mg/L. Consequently, after adsorption for various times, the Pb(II) content in the aqueous solution was detected at each time point separately. As shown in Figure 5A, initially, the adsorbents possessed a surplus of adsorption sites that caused a swift rise in the adsorption capacity of the PVA/PAA/DMTD ENFM for Pb(II) ions within the first 60 min. Subsequently, the process progressively slowed down, reaching adsorption saturation at approximately 180 min. Notably, the equilibrium adsorption capacity of the PVA/PAA/DMTD ENFM for Pb(II) ions was 14.1 mg/g, indicating a 3.1-fold increase compared with the PVA/PAA ENFM (Figure S3A).

As illustrated in Figure 5B, the adsorption performance of the PVA/PAA/DMTD ENFM was also subject to the influence of the starting level of Pb(II) ions. At a relatively low level of Pb(II), they were entirely bound to the effective binding sites of the adsorbents. However, when the starting concentration was approximately 60–100 mg/L, the adsorption capacity of the PVA/PAA/DMTD ENFM for Pb(II) was unchanged because of the saturation of the adsorption sites. At an initial Pb(II) content of 60 mg/L, the adsorption capacity of the PVA/PAA/DMTD ENFM reached 138.3 mg/g, surpassing the maximum equilibrium adsorption capacity of the PVA/PAA ENFM that was approximately 21.1 mg/g (Figure S3B).

## Adsorption kinetics

Kinetic models are mathematical expressions for $q_t$ as a function of time when the initial concentration is pre-specified.[36] As illustrated in Figures 6A–6C and Table 1, the coefficients of determination ($R^2$) close to one demonstrated that the experimental data were well fitted

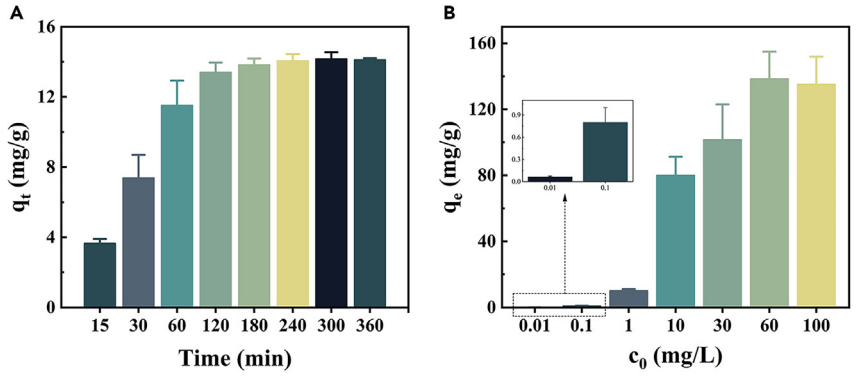


**Figure 5. Effect of adsorption conditions**

The impact of (A) the adsorption time and (B) starting concentration on the adsorption capacity of the PVA/PAA/DMTD ENFM for Pb(II) ions.
Data are represented as means ± SDs, n = 3.

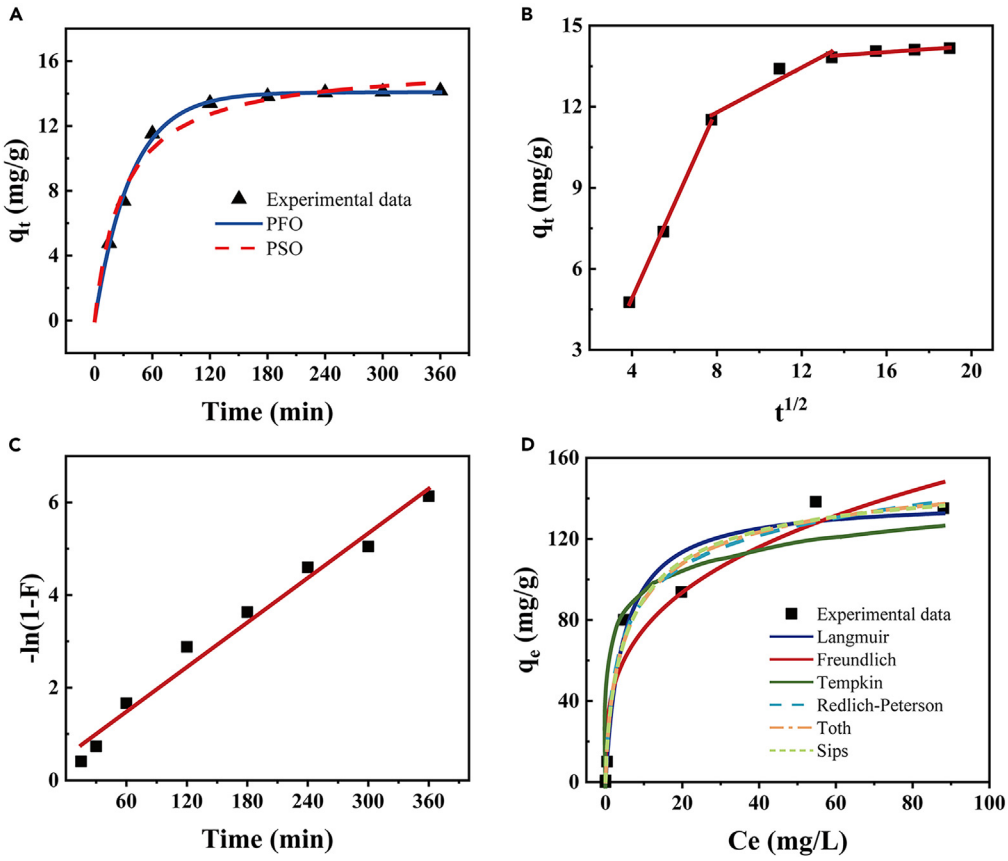


**Figure 6. Adsorption kinetics and adsorption isotherms model fitting curves of the PVA/PAA/DMTD ENFM**

(A) pseudo-first-order (PFO) and pseudo-second-order (PSO) model fit with experimental data, respectively; (B) Weber-Morris intraparticle diffusion model; (C) Boyd's external-diffusion model; and (D) various isotherm models fit with experimental.

to the adsorption kinetic models. However, by comparing the values of $R^2$, we could not absolutely identify whether the pseudo second order (PSO) model or the pseudo first order (PFO) model was the best-fitting model. Nevertheless, when the initial concentration was 1 mg/L, the $q_m$ value predicted by the PFO model was very close to the experimental value (14.1 mg/g) compared with the other kinetic models. Therefore, the PFO model was the best kinetic model to explain the adsorption of lead ions on the PVA/PAA/DMTD ENFM.[37]

The experimental data were fitted to Boyd's external diffusion equation and the Weber-Morris internal diffusion equation to capture whether mass transfer from the liquid film surrounding the adsorbent or diffusion into the internal porous structure of the material was the rate-controlling phase of the adsorption process.[38] To assess the potential for transport of Pb(II) ions within the pores of the fiber membranes, the adsorption data were fitted to the intraparticle diffusion plots. The intraparticle diffusion model is typically given by the Weber-Morris equation.[39] The plot of $q_t$ versus $t^{1/2}$ is not a straight line and does not pass through (0, 0), indicating that adsorption was controlled by more than one process.[38] Boyd's external diffusion showed a high goodness of fit to the experimental results not only through a high $R^2$ value but also through an intercept close to zero. Such results demonstrated that film diffusion was the rate-controlling phase.[37]

## Isothermal studies

Adsorption equilibrium studies use several isothermal models in the form of $q_e = F(Ce)$ functions. The adsorption isotherms of Pb(II) by the PVA/PAA/DMTD ENFM were investigated at a temperature of 298 K. To find the best isotherm model for interpreting the data reported in these plots, three two-parameter models (Langmuir, Freundlich, and Tempkin) and three three-parameter models (Redlich-Peterson, Toth, and Sips) were used to fit the experimental data and characterize the possible mechanisms of adsorption of Pb(II) by the PVA/PAA/DMTD.[40] The results are shown in Figure 6D and Table 2. Compared with the Freundlich and Tempkin model, the $R^2$ of the Langmuir model was higher, and the $q_m$ for the Pb(II) ions predicted by the Langmuir model was 138.8 mg/g, which is similar to the experimental data (138.3 mg/g). This implied that the Langmuir model was more suitable for the Pb(II) adsorption process by the PVA/PAA/DMTD ENFM. Therefore, the process of Pb(II) ions adsorption by the PVA/PAA/DMTD ENFM may follow a monolayer adsorption mechanism.[41]

**Table 1. Parameters of the adsorption kinetics for Pb(II) ion uptake onto the PVA/PAA/DMTD ENFM**

| Kinetics model | Equation | Parameters | | $R^2$ |
|---|---|---|---|---|
| Pseudo-first-order | $q_t = q_e \cdot [1 - \exp(-k_1 t)]$ | $k_1$ ($min^{-1}$) | $q_e$ ($mg \cdot g^{-1}$) | 0.999 |
| | | 0.026 | 14.1 | |
| Pseudo-second-order | $q_t = q_e^2 k_2 t / [k_2 q_e t + 1]$ | $k_2$ ($g \cdot mg^{-1} \cdot min^{-1}$) | $q_e$ ($mg \cdot g^{-1}$) | 0.989 |
| | | 0.002 | 15.9 | |
| Weber-Morris | $q_t = k_{ip} t^{1/2} + I$ | $k_{ip1}$ ($mg \cdot g^{-1} \cdot min^{-1/2}$) | $I_1$ | 0.998 |
| | | 1.75 | −2.08 | |
| | | $k_{ip2}$ ($mg \cdot g^{-1} \cdot min^{-1/2}$) | $I_2$ | 0.925 |
| | | 0.42 | 8.46 | |
| | | $k_{ip3}$ ($mg \cdot g^{-1} \cdot min^{-1/2}$) | $I_3$ | 0.729 |
| | | 0.05 | 13.2 | |
| Boyd | $-\ln(1 - F) = k_b + A$; $F = \frac{q_t}{q_e}$ | $k_b$ ($min^{-1}$) | A | 0.979 |
| | | 0.016 | 0.52 | |

Similarly, the adsorption isotherms all followed the three-parameter models of Redlich-Peterson, Toth, and Sips. However, the values of n in the three-parameter models were not near one, and this indicated that the adsorption sites of Pb(II) in the PVA/PAA/DMTD ENFM were not homogeneous.[42,43]

The Pb(II) ion adsorption performance of the PVA/PAA/DMTD ENFM was compared with those of electrospun nanofibrous membranes reported previously to evaluate its adsorption performance. Table 3 shows the $q_m$ values of various electrospun nanofibrous membranes for Pb(II) ions reported in some recent studies. Compared with other electrospun membranes, the PVA/PAA/DMTD ENFMs had a relatively excellent adsorption capacity for Pb(II) ions. Although the adsorption capacity of the PVA/PAA/DMTD ENFM was slightly lower than that of some ENFMs,[44,45] the operating method is more convenient and the materials are safer because we used an aqueous polymer solution for electrospinning and cross-linking by heat treatment, a process that does not involve organic solvents or cross-linking agents. These results indicated that the PVA/PAA/DMTD ENFM material showed better application potential for the elimination of Pb(II) ions from water and liquid foods.

## Effect of temperature and thermodynamic study

Changes in temperature may result in changes in the adsorption capacity and equilibrium constant of an adsorbent. As shown in Figure 7A, the adsorption capacity of the PVA/PAA/DMTD ENFM for Pb(II) increased with increasing temperature. The increase in the adsorption capacity may have been due to an increase in the adsorption equilibrium constant at a higher temperature. To assess the feasibility and

**Table 2. Parameters of the adsorption isotherms for Pb(II) ion uptake onto the PVA/PAA/DMTD ENFM**

| Isotherms model | Equation | Parameters | | | $R^2$ |
|---|---|---|---|---|---|
| Langmuir | $q_e = q_m b_L c_e / (1 + b_L c_e)$ | $q_m$ ($mg \cdot g^{-1}$) | | $b_L$ ($L \cdot mg^{-1}$) | 0.982 |
| | | 138.8 | | 0.9 | |
| Freundlich | $q_e = b_F c_e^{1/n}$ | $b_F$ ($mg^{1-1/n} \cdot L^{1/n} \cdot g^{-1}$) | | n | 0.950 |
| | | 37.3 | | 3.2 | |
| Tempkin | $q_e = \frac{RT}{b}(\ln k c_e)$; $B = \frac{RT}{b}$ | k ($L \cdot mg^{-1}$) | | B | 0.879 |
| | | 50.5 | | 15.1 | |
| Redlich-Peterson | $q_e = k_R c_e / (1 + a_R c_e^n)$ | $k_R$ ($L \cdot mg^{-1}$) | n | $a_R$ | 0.974 |
| | | 53.6 | 0.87 | 0.7 | |
| Toth | $q_e = \frac{q_m k_T c_e}{[1+(k_T c_e)^n]^{1/n}}$ | $k_T$ ($mg \cdot L^{-1}$) | n | $q_m$ ($mg \cdot g^{-1}$) | 0.971 |
| | | 0.43 | 0.58 | 167.9 | |
| Sips | $q_e = \frac{q_m (k_s c_e)^n}{1+(k_s c_e)^n}$ | $k_s$ ($L^{1/n} \cdot mg^{-1/n}$) | n | $q_m$ ($mg \cdot g^{-1}$) | 0.968 |
| | | 0.15 | 0.75 | 155.5 | |

**Table 3. Comparison of the adsorption performances for Pb(II) on other electrospun nanofibrous membranes**

| ENFM | Abbreviation | $q_m$ (mg/g) | Cycle number | Solvents | Cross-linking agents | Reference |
|---|---|---|---|---|---|---|
| Multiwalled carbon nanotube—Polyethyleneimine/Polyacrylonitrile | MWCNT-PEI/PAN | 232.7 | 5 | N, N-dimethylformamide[b] | / | Deng et al.[44] |
| Chitosan/Poly(ethylene oxide) | CS/PEO | 108 | 5 | Acetic acid[a] | / | Shariful et al.[46] |
| Polyethyleneimine/Polyvinyl alcohol | PEI/PVA | 90.03 | 3 | Distilled water | N,N-dimethylformamide[b], glutaraldehyde[c] | Wang et al.[47] |
| Poly(ether sulfones)/Poly(ethyleneimine) | PES/PEI | 94.34 | 3 | N, N-dimethylacetamide[d] | Glutaraldehyde[c], acetone[d] | Min et al.[48] |
| Cellulose acetate/Polymethacrylic acid | CA/PMAA | 146.21 | 5 | N, N-dimethylformamide[b] | / | Zang et al.[45] |
| Phosphorylated polyacrylonitrile | P-PAN | 98.06 | 4 | N, N-dimethylformamide[b] | Hydrazine hydrate[e] | Zhao et al.[49] |
| Polyurethane/Phytic acid | PU/PA | 136.52 | 5 | N, N-dimethylformamide[b], tetrahydrofuran[f] | / | Fang et al.[50] |
| Poly(vinyl) alcohol/poly(acrylic) acid/2,5-dimercapto-1,3,4-thiadiazole | PVA/PAA/DMTD | 138.79 | 6 | Distilled water | / | This study |

GHS classification:
[a]Flammable liquids (Category 3), H226; Skin corrosion/irritation (Category 1A), H314; Serious eye damage/eye irritation (Category 1), H318.
[b]Acute toxicity, Dermal (Category 4), H312; Serious eye damage/eye irritation (Category 2A), H319; Acute toxicity, Inhalation (Category 4), H332; Reproductive toxicity (Category 1B), H360.
[c]Acute toxicity, oral (Category 3), H301; Skin corrosion/irritation (Category 1B), H314; Skin sensitization (Category 1), H317; Acute toxicity, inhalation (Category 1), H330; Respiratory sensitization (Category 1), H334; Specific target organ toxicity—single exposure, respiratory tract irritation (Category 3), H335; Short-term (acute) aquatic hazard (Category 1), H400; Long-term (chronic) aquatic hazard (Category 2), H411.
[d]Flammable liquids (Category 2), H225; Serious eye damage/eye irritation (Category 2A), H319; Specific target organ toxicity—single exposure (Category 3), Narcotic effects, H336.
[e]Flammable liquids (Category 3), H226; Acute toxicity, oral (Category 3), H301; Acute toxicity, inhalation (Category 2), H330; Acute toxicity, dermal (Category 3), H311; Skin corrosion/irritation (Category 1B), H314; Skin sensitization (Category 1), H317; Carcinogenicity (Category 1B), H350; Short-term (acute) aquatic hazard (Category 1), H400; Long-term (chronic) aquatic hazard (Category 1), H410.
[f]Flammable liquids (Category 2), H225; Serious eye damage/eye irritation (Category 2A), H319; Specific target organ toxicity—single exposure, respiratory tract irritation (Category 3), H335; Carcinogenicity (Category 2), H351.

spontaneity of the adsorption process, the slopes and intercepts of van't Hoff equation were used to evaluate the changes in free energy ($\Delta G^\circ$), enthalpy ($\Delta H^\circ$), and entropy ($\Delta S^\circ$).[51]

$$\ln b_L = -\frac{\Delta H^\circ}{RT} + \frac{\Delta S^\circ}{R} \quad \text{(Equation 1)}$$

$$\Delta G^\circ = -RT \ln b_L \quad \text{(Equation 2)}$$

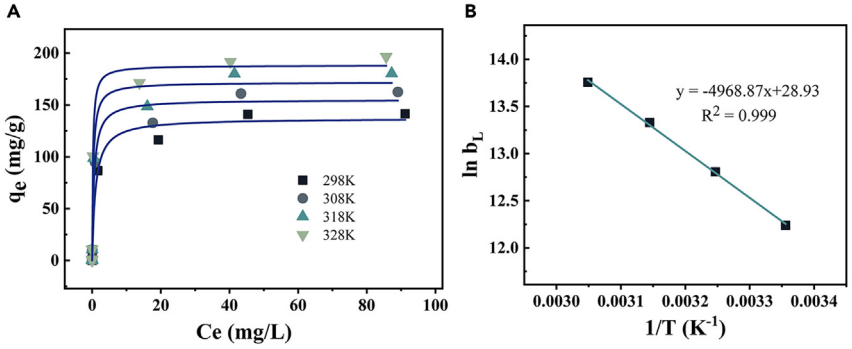


**Figure 7. Effect of temperature and thermodynamic study**
(A) Effect of temperature on the adsorption properties of the PVA/PAA/DMTD ENFM and Langmuir model fitting and (B) the linear fit of the ln $b_L$ to 1/T for determining the thermodynamic parameters.

**Table 4. Thermodynamic parameters of the adsorption of Pb(II) by the PVA/PAA/DMTD ENFM**

| T (K) | $b_L$ (L·mol$^{-1}$) | $\Delta G^\circ$(kJ·mol$^{-1}$) | $\Delta H^\circ$ (kJ·mol$^{-1}$) | $\Delta S^\circ$ (kJ·mol$^{-1}$·K$^{-1}$) |
|---|---|---|---|---|
| 298 | $2.07\times10^4$ | −30.36 | 41.31 | 0.24 |
| 308 | $3.65\times10^4$ | −32.77 | | |
| 318 | $6.15\times10^4$ | −35.18 | | |
| 328 | $9.43\times10^4$ | −37.58 | | |

where $b_L$ (L·mol$^{-1}$) is the Langmuir equilibrium constant; T (K) is the temperature; $\Delta H^\circ$ (kJ·mol$^{-1}$) is the standard enthalpy change; $\Delta S^\circ$ (kJ·mol$^{-1}$· K$^{-1}$) is the standard entropy change; $\Delta G^\circ$ (kJ·mol$^{-1}$) is the standard Gibbs free energy change; and R is the gas constant (8.314 J·mol$^{-1}$ ·K$^{-1}$).

As shown in Figure 7B, the values of $\Delta S^\circ$ and $\Delta H^\circ$ were estimated based on vant Hoff's equation, plotted with the ln $b_L$ with respect to 1/T, and based on the slope and intercept, which were 0.24 kJ·mol$^{-1}$·K$^{-1}$ and 41.31 kJ·mol$^{-1}$, respectively. Additionally, $\Delta G^\circ$ was calculated according to Equation 5 for different temperatures, as shown in Table 4. Positive values of $\Delta H^\circ$ indicate an endothermic nature of the adsorption process. The range of $\Delta H^\circ$ for hydrogen-bonding forces is typically between 2 and 40 kJ·mol$^{-1}$, so if $\Delta H^\circ$<40 kJ·mol$^{-1}$, physisorption is considered to have occurred. We calculated the $\Delta H^\circ$ was 41.31 kJ·mol$^{-1}$, which is near the threshold value. Hence, it can be concluded that the process of Pb(II) adsorption by the PVA/PAA/DMTD ENFM was primarily physical. Negative values of the $\Delta G^\circ$ (−30.36, −32.77, −35.18, and −37.58 kJ·mol$^{-1}$) indicated the feasibility and spontaneity of the adsorption process at 298, 308, 318, and 328 K. The $\Delta S^\circ$ exhibited a positive value, and this indicated an augmentation in disorder at the solid/solution interface during the adsorption of Pb(II). This positive $\Delta S^\circ$ value was attributed to the expansion of system stoichiometry that resulted from the desorption of hydrated water.[52]

## Selectivity and recyclability of the PVA/PAA/DMTD ENFM

In contrast to some previous studies, which have focused solely on Pb(II) removal from environmental water, it is crucial to examine the impact of adsorbents on other essential metal ions in liquid foods. Figure 8A shows that when the concentrations of metal ions were all 10 mg/L, the equilibrium adsorption capacity of the PVA/PAA/DMTD ENFM for Pb(II) reached 116.1 mg/g, a significantly greater value compared with that of the other metal ions (Zn(II) ions [47.3 mg/g], Ca(II) ions [42.8 mg/g], Fe(III) ions [22.1 mg/g], Cd(II) ions [26.7 mg/g], K(I) ions [12.5 mg/g], and Mg(II) [0.9 mg/g]).

To better simulate real-world application scenarios, adsorption experiments were performed on mixed metal solutions using the PVA/PAA/DMTD ENFM to test the ability of the materials to selectively adsorb lead ions. The adsorption efficiency for Pb(II) was as high as 51.0% in a mixed metal cations solution, whereas the adsorption efficiency of the PVA/PAA/DMTD ENFM for other metal ions ranged from 4.1%–7.4% (Figure 8B). By referring to other studies, we calculated the selectivity factors according to Equation 3:[53]

$$\alpha_M^{Pb} = \frac{D_{Pb}}{D_M} \text{ where } D = \frac{q_e}{c_e} \quad \text{(Equation 3)}$$

where $\alpha$ is the selectivity factor, D is the distribution ratio, and the subscript M indicates a metal ion other than Pb(II) in the mixture.

As shown in Table 5, these data indicated the excellent selectivity of the PVA/PAA/DMTD ENFM toward Pb(II) and minimal impact on the concentration of essential metal elements in liquid food beneficial to human health. Some adsorbents studied in the past may affect Ca(II),[54] Zn(II),[46] and other ions while adsorbing heavy metal Pb(II). However, the PVA/PAA/DMTD ENFM exhibited high specificity to Pb(II) ions and minimized the impact on other essential metal elements, demonstrating its significant practical value in maintaining the nutritional content of liquid food.

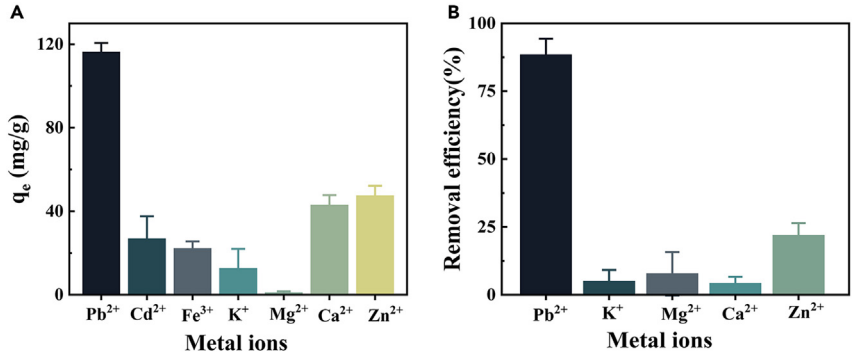


**Figure 8. Selectivity of PVA/PAA/DMTD ENFM**

Selective adsorption of Pb(II) ions in (A) separate metal ions and (B) mixed metal ions by the PVA/PAA/DMTD ENFM. Data are represented as means ± SDs, n = 3.

**Table 5. The selectivity factor values of the PVA/PAA/DMTD ENFM for Pb(II) with respect to several other metal ions in the mixture**

| Metal ion | Pb(II) | K(I) | Mg(II) | Ca(II) | Zn(II) |
|---|---|---|---|---|---|
| $D_{Pb}$ | 15.60 | – | – | – | – |
| $D_M$ | – | 1.08 | 0.63 | 1.20 | 0.95 |
| $\alpha_M^{Pb}$ | – | 14.49 | 24.72 | 13.00 | 16.40 |

The reusability of the PVA/PAA/DMTD ENFM was assessed through continuous adsorption–desorption cycles, which is crucial for the practical application potential of ENFM.[55] The removal efficiency decreased from 98.9% to 98.0% after six cycles of adsorption/desorption, corresponding to 99.1% of the initial removal efficiency for Pb(II) ions (Figure 9). Some previous studies had reported that the removal efficiency MWCNT-PEI/PAN ENFM for Pb(II) ions dropped by approximately 17% after five cycles of adsorption and desorption.[44] Compared with these materials, the PVA/PAA/DMTD ENFM maintained its effective adsorption properties for Pb(II) ions even after repeated use.

## Adsorption mechanism

The X-ray photoelectron spectroscopy (XPS) technique was employed to further investigate the mechanism for the adsorption of Pb(II) to PVA/PAA/DMTD ENFM. The wide-scan XPS spectra of the PVA/PAA/DMTD ENFM before and after treatment of Pb(II) are given in Figures 10A and 10B, which clearly shows the existence of Pb 4f peak, demonstrating that adsorption of Pb(II) occurred in this material. Figures 10C and 10D show the S2p spectra before and after Pb(II) adsorption on the PVA/PAA/DMTD ENFM. The S2p peaks were slightly shifted after Pb(II) adsorption on the fibrous membrane, and the binding energies increased from 169.81, 168.60, 163.98, and 161.98 eV to 169.88, 168.64, 164.26, and 162.13 eV, respectively, which indicated that the S in the DMTD on the surface of the ENFM was involved in the adsorption process of Pb(II) ions. The N1s and O1s spectra of PVA/PAA/DMTD ENFM before and after treatment of Pb(II) are shown in Figures 10E–10H, which show that the = N- in N1s also shifted to low binding energy after adsorption, indicating that = N- of the DMTD also participated in the adsorption. The removal mechanism can be attributed to strong coordination interaction between multiple adsorption sites and Pb(II) in which the synergism of sulfur- and nitrogen-containing functional groups in the DMTD played an important role in the removal of Pb(II).

## Practical application of the PVA/PAA/DMTD ENFM in non-alcoholic beverages and liquor

Spring water was spiked with Pb(II) ions at concentrations of 0, 5, 10, 50, 100, and 500 μg/L. Following a 3-h adsorption process using the PVA/PAA/DMTD ENFM, the concentrations of Pb(II) ions in the samples were quantified using ICP-MS after preprocessing. In the original spring water, the concentration of Pb(II) was approximately 1.72 ± 0.57 μg/L. When the Pb(II) ions were not artificially added, the PVA/PAA/DMTD ENFM slightly reduced the Pb(II) content in it (Figure 11A). In fact, the concentration of Pb(II) in the spring water remained below the Chinese national standard of 10 μg/L, even with the addition of 5 μg/L lead(II) ions. However, the adsorbent showed effective adsorption performance in spring water, with a removal efficiency exceeding 70% across the Pb(II) ions concentrations spanning from 5 to 500 μg/L (Figure 11B). Moreover, the use of the PVA/PAA/DMTD ENFM further reduced the concentration of Pb(II). Additionally, Figure 12A illustrates that the adsorption

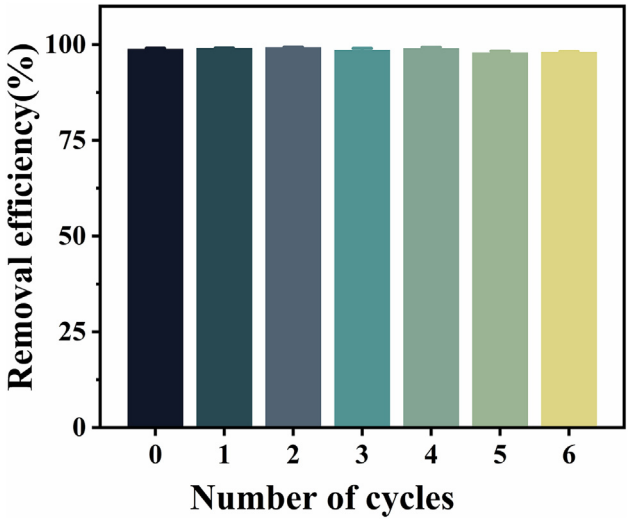


**Figure 9. Effect of the number of regeneration cycles on Pb(II) ion adsorption by the PVA/PAA/DMTD ENFM**
Data are represented as means ± SDs, n = 3.

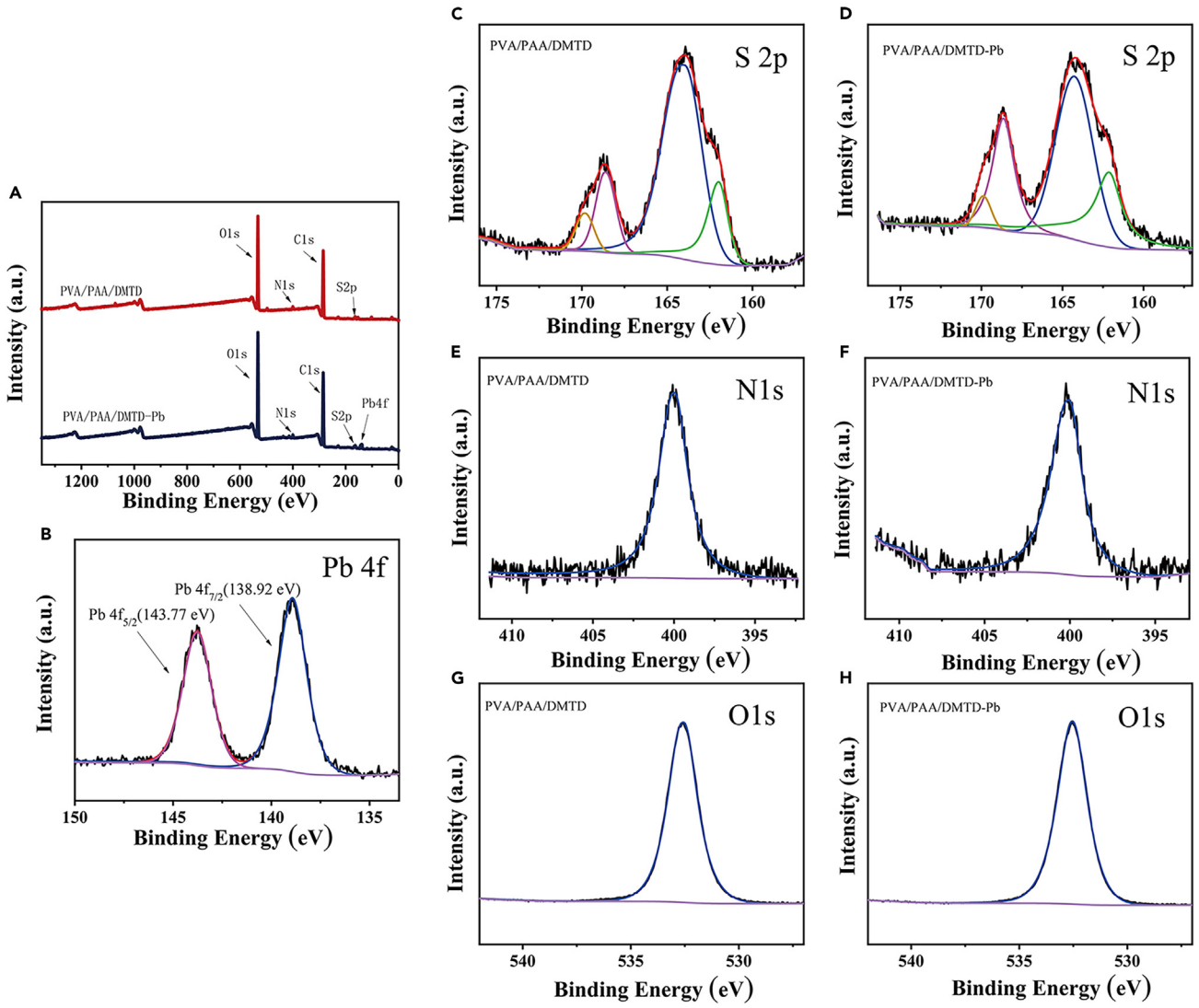


**Figure 10. The mechanism for the adsorption of Pb(II) to PVA/PAA/DMTD ENFM**

(A) Full scan survey XPS spectra of the PVA/PAA/DMTD ENFM before and after Pb(II) adsorption; (B) XPS Pb 4f spectra of the PVA/PAA/DMTD ENFM after Pb(II) adsorption; (C and D) S 2p, (E and F) N 1s, and (G and H) O 1s spectra of the PVA/PAA/DMTD ENFM before and after Pb(II) adsorption.

performance of $Pb^{2+}$ in spring water by the PVA/PAA/DMTD ENFM had minimal impact on the levels of $Mg^{2+}$, $K^{+}$, $Ca^{2+}$, and $Zn^{2+}$. The removal of Pb(II) using the PVA/PAA/DMTD ENFM was investigated in green tea drinks spiked with Pb(II) at various concentrations of 0, 5, 10, 50, 100, and 500 μg/L. Figures 11A and 11C illustrate the removal efficiency and adsorption capacity of the PVA/PAA/DMTD ENFM for Pb(II) in green tea drinks. In the absence of added lead(II), the content of Pb(II) in the green tea drinks was approximately 21.99 ± 3.62 μg/L. When extra Pb(II) ions were not added, the PVA/PAA/DMTD ENFM reduced approximately 50% of the Pb(II) content. In green tea beverages contaminated with simulated Pb(II) at concentrations of 5, 10, 50, 100, and 500 μg/L, the use of the PVA/PAA/DMTD ENFM demonstrated substantial removal of Pb(II), with removal efficiencies ranging from approximately 50%–80%. Despite being lower than the Chinese national standard of 300 μg/L, the content of Pb(II) was further reduced. The levels of TPP, as well as $Mg^{2+}$, $K^{+}$, $Ca^{2+}$, and $Zn^{2+}$ in the beverage, were examined before and after adsorption. Figure 12B illustrates that the PVA/PAA/DMTD ENFM had minimal impact on the Pb(II) adsorption process in green tea drinks.

Baijiu samples were spiked with Pb(II) at concentrations of 0, 5, 10, 50, 100, and 500 μg/L to evaluate the efficacy of the PVA/PAA/DMTD ENFM for Pb(II) removal. Without the addition of lead(II), the level of Pb(II) in Baijiu was approximately 1.21 ± 0.027 μg/L. Figure 11A illustrates that the PVA/PAA/DMTD ENFM was capable of effectively reducing the content of lead(II) ions in Baijiu, even in the absence of additional lead(II) ions. Figure 11D shows the simulated contamination of Baijiu with Pb(II) at concentrations of 5, 10, 50, 100, and 500 μg/L, and the application of the PVA/PAA/DMTD ENFM exhibited notable efficiency in removing Pb(II), with removal efficiencies ranging from approximately

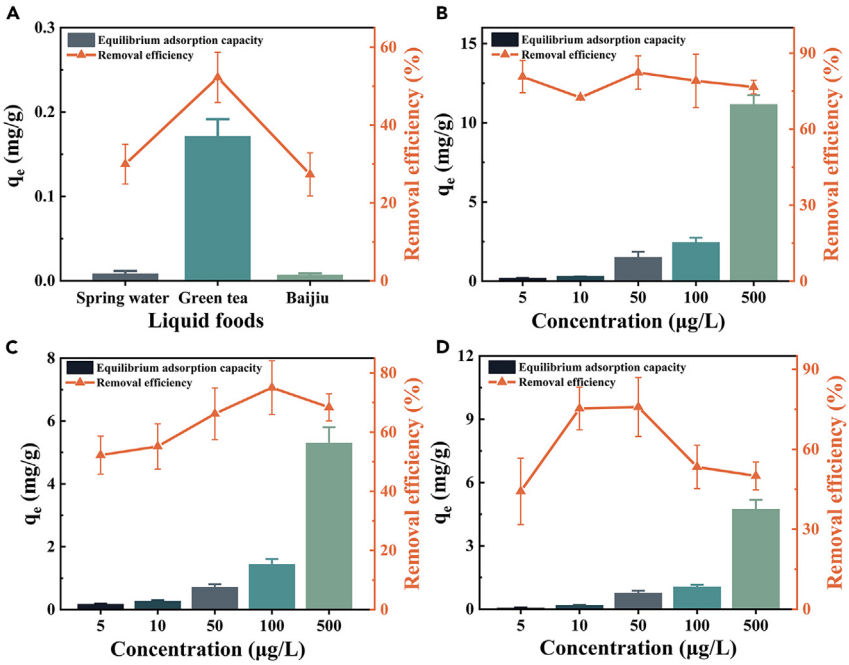


**Figure 11. Practical application of the PVA/PAA/DMTD ENFM**

(A) Adsorption performance of the PVA/PAA/DMTD ENFM for Pb(II) in different liquid foods without adding Pb(II) ions and in (B) spring water, (C) green tea drinks, and (D) Baijiu when different concentrations of Pb(II) ions were added. Data are represented as means ± SDs, n = 3.

40%–80%. Moreover, the addition of 5, 10, 50, and 100 μg/L of Pb(II) to the Baijiu resulted in Pb(II) concentrations well below the Chinese national standard of 500 μg/L, demonstrating the ability of the PVA/PAA/DMTD ENFM to effectively lower the Pb(II) content in Baijiu, even when initial levels were already below the standard. Additionally, as shown in Figure 12C, the PVA/PAA/DMTD ENFM exhibited favorable selectivity toward Pb(II) in Baijiu, and the levels of $K^+$, $Ca^{2+}$, $Mg^{2+}$, and $Zn^{2+}$ remained largely unaltered when the Pb(II) ions were removed.

Overall, the PVA/PAA/DMTD ENFM effectively reduced Pb(II) ions in some liquid foods with little impact on the content of beneficial metal ions, which proved the feasibility of its practical application. Nevertheless, the findings indicated that the removal efficiency of Pb(II) ions in actual liquid foods was marginally lower compared with aqueous solutions in the batch adsorption experiments. This decline probably was explained by the existence of other ions in the actual liquid food samples that may be in competition with Pb(II) for active adsorption sites.[56] Additionally, organic compounds, such as tea polyphenols, pigments, esters, polysaccharides, alcohols, and organic acids, are found in liquid foods. These substances have the potential to affect the functional groups present on the adsorption materials, potentially causing the occupation of adsorption sites on the PVA/PAA/DMTD ENFM.[35] This could also explain why we observed that the PVA/PAA/DMTD ENFM did not

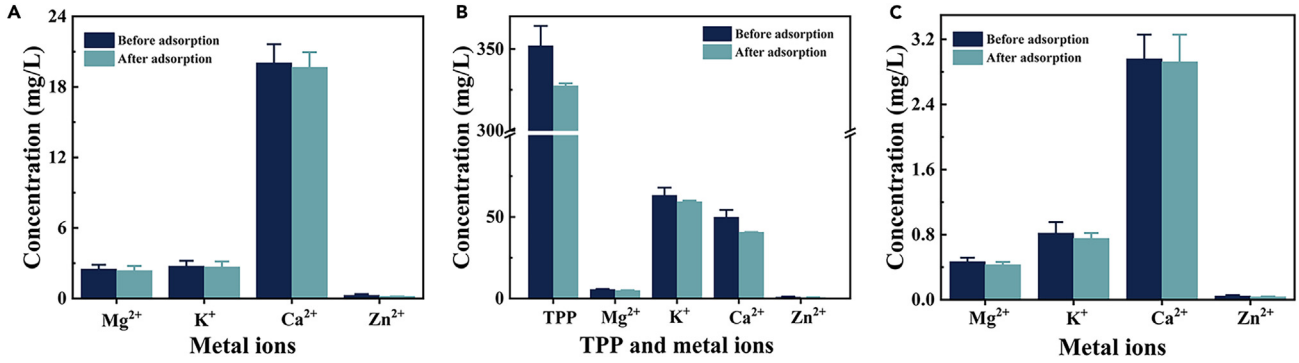


**Figure 12. Interference of PVA/PAA/DMTD ENFM on beneficial components of liquid foods**

Concentration of TPP, $Mg^{2+}$, $K^+$, $Ca^{2+}$, and $Zn^{2+}$ in (A) spring water, (B) green tea drinks, and (C) Baijiu before and after adsorption of Pb(II) ions by the PVA/PAA/DMTD ENFM. Data are represented as means ± SDs, n = 3.

remove Pb(II) as effectively in green tea drinks and Baijiu as it did in spring water. Although the removability of Pb(II) ions by the PVA/PAA/DMTD ENFM in real liquid food was somewhat affected, it still demonstrated a good adsorption capacity. The PVA/PAA/DMTD ENFM exhibited excellent selectivity for Pb(II) ions while having minimal impact on other beneficial ingredients. Furthermore, the PVA/PAA/DMTD ENFM effectively removed Pb(II) ions directly from actual liquid food products, even when the amount was within the limits specified by national standards. Consequently, it holds promise as a prospective adsorbent for the effective elimination of Pb(II) ions from water and liquid foods.

## Conclusion

In summary, we successfully constructed an electrospun fibrous membrane (PVA/PAA/DMTD ENFM) that demonstrates efficiency and selectivity in removing Pb(II) ions. The inclusion of DMTD molecules significantly enhanced the adsorption ability for Pb(II) ions. The PVA/PAA/DMTD ENFM attained an equilibrium adsorption capacity of 138.3 mg/g, compared with approximately 21.1 mg/g for the PVA/PAA ENFM. The PVA/PAA/DMTD ENFM demonstrated a remarkable removal efficiency exceeding 98% for Pb(II) ions. Even after six adsorption/desorption cycles, the removal efficiency for lead(II) ions persisted at 99.1% of the initial amount. The capacity for multiple cycles of reuse without substantial loss suggests the practicality and cost-effectiveness of these materials. When exposed to mixed metal ion solutions, the adsorption efficiencies of the PVA/PAA/DMTD ENFM toward $K^+$, $Ca^{2+}$, $Mg^{2+}$, and $Zn^{2+}$ were only in the range of 4.1%–7.4%. These results suggest that the adsorbent has minimal impact on essential metal elements that are beneficial to human health that are present in liquid foods.

Remarkably, the PVA/PAA/DMTD ENFM demonstrated successful application in removing Pb(II) ions from bottled beverages, including spring water, green tea drinks, and Baijiu. When these liquid foods contained low concentrations of lead(II) ions (5–500 μg/L), employing the PVA/PAA/DMTD ENFM resulted in the removal of over 40% of the Pb(II), with a particularly high removal efficiency observed in spring water (70%–90%). Therefore, this adsorbent exhibits considerable potential for removing Pb(II) ions, a harmful heavy metal, from liquid food products.

## Limitations of the study

In this study, PVA/PAA/DMTD ENFM was prepared, which provides a new strategy for the development of adsorbents for heavy metal Pb(II) in liquid foods. However, this study also has limitations. The stability of the adsorbent in liquid foods with complex matrices has yet to be confirmed. In addition, the PVA/PAA/DMTD ENFM can only be used for the removal of Pb(II) ions from liquid foods, and in the future it will be necessary to develop materials for the rapid removal of heavy metals from a wider range of solid foods.

## STAR★METHODS

Detailed methods are provided in the online version of this paper and include the following:

- KEY RESOURCES TABLE
- RESOURCE AVAILABILITY
  - Lead contact
  - Materials availability
  - Data and code availability
- METHOD DETAILS
  - Chemicals and materials
  - Preparation of the electrospun nanofibrous membrane (ENFM)
  - Adsorption experiments in an aqueous solution
  - Practical application
- QUANTIFICATION AND STATISTICAL ANALYSIS

## SUPPLEMENTAL INFORMATION

Supplemental information can be found online at https://doi.org/10.1016/j.isci.2023.108737.

## ACKNOWLEDGMENTS

This study was supported and funded by the National Key R&D Program of China (2019YFC1604603), the National Natural Science Foundation of China (52103328), the Guangdong Basic and Applied Basic Research Foundation (2020A1515110575), and the Guangzhou Municipal Science and Technology Bureau (202102020422). We thank LetPub (www.letpub.com) for its linguistic assistance during the preparation of this manuscript.

## AUTHOR CONTRIBUTIONS

Conceptualization, Q.W. and Y.Z.; methodology, H.W., D.M., Q.W., and Y.Z.; resources, Q.W. and Y.Z.; data curation, Y.Y., Z.Z., H.W., and D.M.; visualization, Y.Y. and Z.Z.; writing—original draft, H.W. and D.M.; writing—review & editing, Q.W. and Y.Z.; funding acquisition, Q.W. and Y.Z; supervision, Q.W., Y.Z., H.W., and D.M.

## DECLARATION OF INTERESTS

The authors declare no competing interests.

Received: August 14, 2023
Revised: August 28, 2023
Accepted: December 12, 2023
Published: December 15, 2023

## REFERENCES

1. Sharma, A., and Nagpal, A.K. (2020). Contamination of vegetables with heavy metals across the globe: hampering food security goal. J. Food Sci. Technol. *57*, 391–403.
2. Kumar, S., Prasad, S., Yadav, K.K., Shrivastava, M., Gupta, N., Nagar, S., Bach, Q.V., Kamyab, H., Khan, S.A., Yadav, S., and Malav, L.C. (2019). Hazardous heavy metals contamination of vegetables and food chain: Role of sustainable remediation approaches - A review. Environ. Res. *179*, 108792.
3. Bleich, S.N., Vercammen, K.A., Koma, J.W., and Li, Z. (2018). Trends in Beverage Consumption Among Children and Adults. Obesity *26*, 432–441.
4. Dai, J., Soto, M.J., Dunn, C.G., and Bleich, S.N. (2021). Trends and patterns in sugar-sweetened beverage consumption among children and adults by race and/or ethnicity, 2003–2018. Public Health Nutr. *24*, 2405–2410.
5. Yan, Y., Yang, S., Zhou, Y., Song, Y., Huang, J., Liu, Z., Wang, Y., and Wei, S. (2020). Estimating the national burden of mild intellectual disability in children exposed to dietary lead in China. Environ. Int. *137*, 105553.
6. Lanphear, B.P., Hornung, R., Khoury, J., Yolton, K., Baghurst, P., Bellinger, D.C., Canfield, R.L., Dietrich, K.N., Bornschein, R., Greene, T., et al. (2005). Low-level environmental lead exposure and children's intellectual function: An international pooled analysis. Environ. Health Perspect. *113*, 894–899.
7. Braun, J.M., Hornung, R., Chen, A., Dietrich, K.N., Jacobs, D.E., Jones, R., Khoury, J.C., Liddy-Hicks, S., Morgan, S., Vanderbeek, S.B., et al. (2018). Effect of Residential Lead-Hazard Interventions on Childhood Blood Lead Concentrations and Neurobehavioral Outcomes: A Randomized Clinical Trial. JAMA Pediatr. *172*, 934–942.
8. Zhang, Y., Zhang, W., Huang, J., Zhong, X., Liu, Y., and Chen, K. (2021). Lead contamination status and assessment of potential risk to human health of commercial foods in Guangzhou City in 2017-2019. Wei Sheng Yan Jiu *50*, 832–836.
9. Izah, S.C., Inyang, I.R., Angaye, T.C.N., and Okowa, I.P. (2016). A Review of Heavy Metal Concentration and Potential Health Implications of Beverages Consumed in Nigeria. Toxics *5*, 1.
10. MFDS (2019). The Recovery Measures of "fruit and Vegetable Juice" Products Exceeding the Lead Standard Were Detected. https://www.mfds.go.kr/brd/m_99/view.do.
11. Alqadami, A.A., Naushad, M., ALOthman, Z.A., Alsuhybani, M., and Algamdi, M. (2020). Excellent adsorptive performance of a new nanocomposite for removal of toxic Pb (II) from aqueous environment: adsorption mechanism and modeling analysis. J. Hazard Mater. *389*, 121896.
12. Heraldy, E., Lestari, W.W., Permatasari, D., and Arimurti, D.D. (2018). Biosorbent from tomato waste and apple juice residue for lead removal. J. Environ. Chem. Eng. *6*, 1201–1208.
13. Carolin, C.F., Kumar, P.S., Saravanan, A., Joshiba, G.J., and Naushad, M. (2017). Efficient techniques for the removal of toxic heavy metals from aquatic environment: A review. J. Environ. Chem. Eng. *5*, 2782–2799.
14. Bolisetty, S., Peydayesh, M., and Mezzenga, R. (2019). Sustainable technologies for water purification from heavy metals: review and analysis. Chem. Soc. Rev. *48*, 463–487.
15. Al-Salman, H.N.K., Falih, M.s., Deab, H.B., Altimari, U.S., Shakier, H.G., Dawood, A.H., Ramadan, M.F., Mahmoud, Z.H., Farhan, M.A., Köten, H., and Kianfar, E. (2023). A study in analytical chemistry of adsorption of heavy metal ions using chitosan/graphene nanocomposites. Case Stud. Chem. Environ. Eng. *8*, 100426.
16. Kyzas, G.Z., Bomis, G., Kosheleva, R.I., Efthimiadou, E.K., Favvas, E.P., Kostoglou, M., and Mitropoulos, A.C. (2019). Nanobubbles effect on heavy metal ions adsorption by activated carbon. Chem. Eng. J. *356*, 91–97.
17. Hong, M., Yu, L., Wang, Y., Zhang, J., Chen, Z., Dong, L., Zan, Q., and Li, R. (2019). Heavy metal adsorption with zeolites: The role of hierarchical pore architecture. Chem. Eng. J. *359*, 363–372.
18. Crini, G., Lichtfouse, E., Wilson, L.D., and Morin-Crini, N. (2019). Conventional and non-conventional adsorbents for wastewater treatment. Environ. Chem. Lett. *17*, 195–213.
19. Pereao, O.K., Bode-Aluko, C., Ndayambaje, G., Fatoba, O., and Petrik, L.F. (2017). Electrospinning: Polymer Nanofibre Adsorbent Applications for Metal Ion Removal. J. Polym. Environ. *25*, 1175–1189.
20. Shaulsky, E., Nejati, S., Boo, C., Perreault, F., Osuji, C.O., and Elimelech, M. (2017). Post-fabrication modification of electrospun nanofiber mats with polymer coating for membrane distillation applications. J. Memb. Sci. *530*, 158–165.
21. Zhu, F., Zheng, Y.M., Zhang, B.G., and Dai, Y.R. (2021). A critical review on the electrospun nanofibrous membranes for the adsorption of heavy metals in water treatment. J. Hazard Mater. *401*, 123608.
22. Mantripragada, S., Obare, S.O., and Zhang, L. (2023). Addressing Short-Chain PFAS Contamination in Water with Nanofibrous Adsorbent/Filter Material from Electrospinning. Acc. Chem. Res. *56*, 1271–1278.
23. Rosli, N., Yahya, W.Z.N., and Wirzal, M.D.H. (2022). Crosslinked chitosan/poly(vinyl alcohol) nanofibers functionalized by ionic liquid for heavy metal ions removal. Int. J. Biol. Macromol. *195*, 132–141.
24. Zhang, S., Shi, Q., Christodoulatos, C., and Meng, X. (2019). Lead and cadmium adsorption by electrospun PVA/PAA nanofibers: Batch, spectroscopic, and modeling study. Chemosphere *233*, 405–413.
25. Xiao, M., Chery, J., and Frey, M.W. (2018). Functionalization of Electrospun Poly(vinyl alcohol) (PVA) Nanofiber Membranes for Selective Chemical Capture. ACS Appl. Nano Mater. *1*, 722–729.
26. Tzvetkova, P., Vassileva, P., and Nickolov, R. (2010). Modified silica gel with 5-amino-1,3,4-thiadiazole-2-thiol for heavy metal ions removal. J. Porous Mater. *17*, 459–463.
27. Fu, L., Wang, S., Lin, G., Zhang, L., Liu, Q., Fang, J., Wei, C., and Liu, G. (2019). Post-functionalization of UiO-66-NH2 by 2,5-Dimercapto-1,3,4-thiadiazole for the high efficient removal of Hg(II) in water. J. Hazard Mater. *368*, 42–51.
28. Shahat, A., Hassan, H.M., Azzazy, H.M., El-Sharkawy, E.A., Abdou, H.M., and Awual, M.R. (2018). Novel hierarchical composite adsorbent for selective lead(II) ions capturing from wastewater samples. Chem. Eng. J. *332*, 377–386.
29. Yang, Y., Zhang, Y., Zheng, H., Zhang, B., Zuo, Q., and Fan, K. (2022). Functionalized dual modification of covalent organic framework for efficient and rapid trace heavy metals removal from drinking water. Chemosphere *290*, 133215.
30. Park, J.-A., Kang, J.-K., Lee, S.-C., and Kim, S.-B. (2017). Electrospun poly (acrylic acid)/poly (vinyl alcohol) nanofibrous adsorbents for Cu (II) removal from industrial plating wastewater. RSC Adv. *7*, 18075–18084.
31. Yu, X., Shen, P., Yin, Z., Wang, L., Wang, H., and Liu, D. (2023). Surface modification of malachite using DMTD and its effect on xanthate adsorption. Colloids Surf., A *679*, 132560.
32. Li, C., Huang, S., Min, C., Du, P., Xia, Y., Yang, C., and Huang, Q. (2017). Highly Productive Synthesis, Characterization, and Fluorescence and Heavy Metal Ion Adsorption Properties of Poly(2,5-dimercapto-1,3,4-thiadiazole) Nanosheets. Polymers *10*, 24.
33. Alfaro De Prá, M.A., Ribeiro-do-Valle, R.M., Maraschin, M., and Veleirinho, B. (2017). Effect of collector design on the morphological properties of polycaprolactone electrospun fibers. Mater. Lett. *193*, 154–157.
34. Qu, J., Tian, X., Jiang, Z., Cao, B., Akindolie, M.S., Hu, Q., Feng, C., Feng, Y., Meng, X., and Zhang, Y. (2020). Multi-component adsorption of Pb(II), Cd(II) and Ni(II) onto microwave-functionalized cellulose: Kinetics, isotherms, thermodynamics, mechanisms and application for electroplating wastewater purification. J. Hazard Mater. *387*, 121718.

35. Yang, W., Cheng, M., Han, Y., Luo, X., Li, C., Tang, W., Yue, T., and Li, Z. (2021). Heavy metal ions' poisoning behavior-inspired etched UiO-66/CTS aerogel for Pb(II) and Cd(II) removal from aqueous and apple juice. J. Hazard Mater. *401*, 123318.
36. Mohammadzadeh, A., Kadhim, M.M., Taban, T.Z., Baigenzhenov, O., Ivanets, A., Lal, B., Kumar, N., and Hosseini-Bandegharaei, A. (2023). Adsorption performance of Enterobacter cloacae towards U(VI) ion and application of Enterobacter cloacae/carbon nanotubes to preconcentration and determination of low-levels of U(VI) in water samples. Chemosphere *311*, 136804.
37. Naseri, A., Abed, Z., Rajabi, M., Lal, B., Asghari, A., Baigenzhenov, O., Arghavani-Beydokhti, S., and Hosseini-Bandegharaei, A. (2023). Use of Chrysosporium/carbon nanotubes for preconcentration of ultra-trace cadmium levels from various samples after extensive studies on its adsorption properties. Chemosphere *335*, 139168.
38. Wang, J., and Guo, X. (2020). Adsorption kinetic models: Physical meanings, applications, and solving methods. J. Hazard Mater. *390*, 122156.
39. Weber, T.W., and Chakravorti, R.K. (1974). Pore and solid diffusion models for fixed-bed adsorbers. AIChE J. *20*, 228–238.
40. Hosseini-Bandegharaei, A., Khamirchi, R., Hekmat-Shoar, R., Rahmani-Sani, A., Rastegar, A., Pajohankia, Z., and Fattahi, E. (2016). Sorption efficiency of three novel extractant-impregnated resins containing vesuvin towards Pb(II) ion: Effect of nitrate and amine functionalization of resin backbone. Colloids Surf., A *504*, 62–74.
41. Ezzati, R. (2020). Derivation of Pseudo-First-Order, Pseudo-Second-Order and Modified Pseudo-First-Order rate equations from Langmuir and Freundlich isotherms for adsorption. Chem. Eng. J. *392*, 123705.
42. Vieira, T., Artifon, S.E.S., Cesco, C.T., Vilela, P.B., Becegato, V.A., and Paulino, A.T. (2021). Chitosan-based hydrogels for the sorption of metals and dyes in water: isothermal, kinetic, and thermodynamic evaluations. Colloid Polym. Sci. *299*, 649–662.
43. Jaafari, J., Barzanouni, H., Mazloomi, S., Amir Abadi Farahani, N., Sharafi, K., Soleimani, P., and Haghighat, G.A. (2020). Effective adsorptive removal of reactive dyes by magnetic chitosan nanoparticles: Kinetic, isothermal studies and response surface methodology. Int. J. Biol. Macromol. *164*, 344–355.
44. Deng, S., Liu, X., Liao, J., Lin, H., and Liu, F. (2019). PEI modified multiwalled carbon nanotube as a novel additive in PAN nanofiber membrane for enhanced removal of heavy metal ions. Chem. Eng. J. *375*, 122086.
45. Zang, L., Lin, R., Dou, T., Wang, L., Ma, J., and Sun, L. (2019). Electrospun superhydrophilic membranes for effective removal of Pb(II) from water. Nanoscale Adv. *1*, 389–394.
46. Shariful, M.I., Sharif, S.B., Lee, J.J.L., Habiba, U., Ang, B.C., and Amalina, M.A. (2017). Adsorption of divalent heavy metal ion by mesoporous-high surface area chitosan/poly (ethylene oxide) nanofibrous membrane. Carbohydr. Polym. *157*, 57–64.
47. Wang, X., Min, M., Liu, Z., Yang, Y., Zhou, Z., Zhu, M., Chen, Y., and Hsiao, B.S. (2011). Poly(ethyleneimine) nanofibrous affinity membrane fabricated via one step wet-electrospinning from poly(vinyl alcohol)-doped poly(ethyleneimine) solution system and its application. J. Memb. Sci. *379*, 191–199.
48. Min, M., Shen, L., Hong, G., Zhu, M., Zhang, Y., Wang, X., Chen, Y., and Hsiao, B.S. (2012). Micro-nano structure poly(ether sulfones)/poly(ethyleneimine) nanofibrous affinity membranes for adsorption of anionic dyes and heavy metal ions in aqueous solution. Chem. Eng. J. *197*, 88–100.
49. Zhao, R., Li, X., Sun, B., Shen, M., Tan, X., Ding, Y., Jiang, Z., and Wang, C. (2015). Preparation of phosphorylated polyacrylonitrile-based nanofiber mat and its application for heavy metal ion removal. Chem. Eng. J. *268*, 290–299.
50. Fang, Y., Liu, X., Wu, X., Tao, X., and Fei, W. (2021). Electrospun polyurethane/phytic acid nanofibrous membrane for high efficient removal of heavy metal ions. Environ. Technol. *42*, 1053–1060.
51. Peiravi-Rivash, O., Mashreghi, M., Baigenzhenov, O., and Hosseini-Bandegharaei, A. (2023). Producing bacterial nano-cellulose and keratin from wastes to synthesize keratin/cellulose nanobiocomposite for removal of dyes and heavy metal ions from waters and wastewaters. Colloids Surf., A *656*, 130355.
52. Pandey, S., Fosso-Kankeu, E., Spiro, M.J., Waanders, F., Kumar, N., Ray, S.S., Kim, J., and Kang, M. (2020). Equilibrium, kinetic, and thermodynamic studies of lead ion adsorption from mine wastewater onto MoS2-clinoptilolite composite. Mater. Today Chem. *18*, 100376.
53. Xu, L., Liu, Y., Wang, J., Tang, Y., and Zhang, Z. (2021). Selective adsorption of Pb2+ and Cu2+ on amino-modified attapulgite: Kinetic, thermal dynamic and DFT studies. J. Hazard Mater. *404*, 124140.
54. Li, C., Ma, H., Venkateswaran, S., and Hsiao, B.S. (2020). Highly efficient and sustainable carboxylated cellulose filters for removal of cationic dyes/heavy metals ions. Chem. Eng. J. *389*, 123458.
55. Lima, D.R., Hosseini-Bandegharaei, A., Thue, P.S., Lima, E.C., de Albuquerque, Y.R., dos Reis, G.S., Umpierres, C.S., Dias, S.L., and Tran, H.N. (2019). Efficient acetaminophen removal from water and hospital effluents treatment by activated carbons derived from Brazil nutshells. Colloids Surf., A *583*, 123966.
56. Ragheb, E., Shamsipur, M., Jalali, F., and Mousavi, F. (2022). Modified magnetic-metal organic framework as a green and efficient adsorbent for removal of heavy metals. J. Environ. Chem. Eng. *10*, 107297.

## STAR★METHODS

### KEY RESOURCES TABLE

| REAGENT or RESOURCE | SOURCE | IDENTIFIER |
|---|---|---|
| Chemicals, peptides, and recombinant proteins | | |
| Poly(acrylic) acid | Macklin | Cat#9003-01-4 |
| poly(vinyl) alcohol | Macklin | Cat#9002-89-5 |
| 2,5-dimercapto-1,3,4-thiadiazole | Macklin | Cat#1072-71-5 |
| $Cd(NO_3)_2·4H_2O$ | Aladdin | Cat#10022-68-1 |
| KCl | Aladdin | Cat# 7447-40-7 |
| $Zn(NO_3)_2·6H_2O$ | Aladdin | Cat# 10196-18-6 |
| $Mg(NO_3)_2·6H_2O$ | Aladdin | Cat#13446-18-9 |
| $Fe(NO_3)_3·9H_2O$ | Aladdin | Cat# 7782-61-8 |
| $Ca(NO_3)_2·4H_2O$ | Aladdin | Cat# 13477-34-4 |
| $Pb(NO_3)_2$ | Aladdin | Cat#10099-74-8 |
| Multi-metal standard solution | o2si | Cat#1023079-8 |
| Nitric acid | Acros Organics | Cat#7697-37-2 |
| Other | | |
| Fourier Transform Infrared Spectrometer | Thermo Scientific | Nicolet Nexus 670 |
| Scanning electron microscope | Hitachi | S-4800 |
| Thermogravimetric Analyzer | NETZSCH | TG209F1 Libra |
| X-ray photoelectron spectroscopy | Thermo Scientific | ESCALab250 |
| Inductively Coupled Plasma Mass Spectrometer | Thermo Scientific | iCAP RQ |
| microwave high-pressure reactor | Milestone | UltraClave |

### RESOURCE AVAILABILITY

#### Lead contact

Further information and requests for resources should be directed to and will be fulfilled by the lead contact, Qing Wang(wangq27@mail.sysu.edu.cn).

#### Materials availability

This study did not generate new unique reagents.

#### Data and code availability

All data reported in this paper will be shared by the lead contact upon request.

This paper does not report original code.

Any additional information required to reanalyze the data reported in this paper is available from the lead contact upon request.

### METHOD DETAILS

#### Chemicals and materials

Except for the metal standard solutions, all chemicals were of analytical grade. Poly(acrylic) acid (PAA, $M_w$= 2,000), poly(vinyl) alcohol (PVA, 87−89 mol% hydrolyzed), and 2,5-dimercapto-1,3,4-thiadiazole (DMTD) were purchased from Macklin (Shanghai, China). $Cd(NO_3)_2·4H_2O$, KCl, $Zn(NO_3)_2·6H_2O$, $Mg(NO_3)_2·6H_2O$, $Fe(NO_3)_3·9H_2O$, and $Ca(NO_3)_2·4H_2O$ were purchased from Aladdin (Shanghai, China). $Fe^{3+}$, $K^+$, $Ca^{2+}$, $Mg^{2+}$, and $Zn^{2+}$ standard solutions (1000 mg/L, 5% $HNO_3$) were purchased from o2si (Charleston, SC, USA). The $Cd^{2+}$ and $Pb^{2+}$ standard solutions (1000 mg/L, 5% $HNO_3$) were purchased from Accustandard (New Haven, CT, USA). Nitric acid (68−70% solution in water) was purchased from Acros Organics (Waltham, MA, USA). Ultrapure water (18.2 MΩ·cm resistivity, Millipore) was utilized throughout all of the experiments. Spring water, green tea drinks, and liquor (Baijiu) were purchased in the supermarket (Guangzhou, China).

### Preparation of the electrospun nanofibrous membrane (ENFM)

According to a previous study,[24] separate aqueoussolutions of PVA and PAA were prepared with concentrations of 10 wt.%. DMTD powders were added to the PVA and PAA mixed solutions, and the PVA, PAA, and DMTD mixed solution was obtained after one hour of stirring. The ENFM was made using the horizontally placed electrospinning setup. We spread a layer of aluminum foil on a rotating mandrel and adjusted the distance from the needle tip to the rotating mandrel to 10 cm. The mixed solution was filled into a 10-mL disposable syringe with a 10-mL capacity, and a blunt stainless steel needle was fitted to the syringe. The loaded syringe was mounted on a horizontal syringe pump running at 0.5 mL/h, while a positive voltage of 17 kV was impressed on the syringe tip. After the fibers were collected from the mandrel and separated from the aluminum foil, they were dried in an oven at 60°C for 12 hours, followed by crosslinking at 140°C for two hours.

### Adsorption experiments in an aqueous solution

The fibrous membranes were cut into sizes of 2×2 $cm^2$ with masses of approximately 2 mg each. The fibrous membranes were introduced into 30-mL solutions with varying concentrations of Pb(II) ions. The pH value was adjusted using either a 0.05 mol/L $HNO_3$ solution or a 0.05 mol/L NaOH aqueous solution. The adsorption behavior of the PVA/PAA/DMTD ENFM towards Pb(II) ions was examined in an aqueous solution with pH values of 2, 3, 4, 5, 6, 7, and 8, adsorption times of 0, 15, 30, 60, 120, 180, 240, 300, and 360 min, various initial Pb(II) concentrations of 0.01, 0.1, 1, 10, 30, 60, and 100 mg/L, and temperatures of 298, 308, 318, and 328 K, separately. Additionally, while investigating the adsorption kinetics, a fixed concentration of Pb(II) at 1 mg/L was maintained during the initial adsorption. Except for the isotherm study, the contact time for all adsorption experiments was set at three hours to confirm the adsorption equilibrium was fully achieved. To investigate the selective adsorption ability of the PVA/PAA/DMTD ENFM to Pb(II), the adsorption experiments were conducted using solutions containing $Pb^{2+}$, $Fe^{3+}$, $Cd^{2+}$, $K^{+}$, $Ca^{2+}$, $Mg^{2+}$, and $Zn^{2+}$ ions at concentrations of 10 mg/L each. Additionally, selective adsorption experiments were conducted in a mixed aqueous solution containing 1 mg/L of $Pb^{2+}$ and 10 mg/L each of $K^{+}$, $Ca^{2+}$, $Mg^{2+}$, and $Zn^{2+}$ to evaluate the selectivity of the PVA/PAA/DMTD ENFM towards Pb(II) in the co-existence of higher concentrations of other competing metal cations. To assess the reusability of the PVA/PAA/DMTD ENFM, the adsorption experiment was conducted in a 1 mg/L Pb(II) aqueous solution. Subsequently, desorption was performed using 0.1M NaOH for one hour to eliminate the Pb(II) ions adsorbed on the PVA/PAA/DMTD ENFM. The concentrations of Pb(II) ions in the solution, both prior to and following adsorption, were assessed through the application of Inductively Coupled Plasma Mass Spectrometer (ICP-MS). The removal efficiencies (R,%) for Pb(II) ions in the solutions were determined using Equation 4:

$$R(\%) = (c_0 - c_e) / c_0 \times 100 \quad \text{(Equation 4)}$$

where $c_0$ ($mg \cdot L^{-1}$) represents the initial concentration of Pb(II) ions, and $c_e$ ($mg \cdot L^{-1}$) represents the Pb(II) ions concentrations in solution after reaching adsorption equilibrium.

Additionally, the adsorption capacity of the fiber membranes for Pb(II) ions was calculated using Equations 5 and 6, as follows:

$$q_t = (c_0 - c_t) / m \times V \quad \text{(Equation 5)}$$

$$q_e = (c_0 - c_e) / m \times V \quad \text{(Equation 6)}$$

where $q_t$ ($mg \cdot g^{-1}$) represents the adsorption capacity at time t (min); $q_e$ ($mg \cdot g^{-1}$) signifies the equilibrium adsorption capacity; $V$ (L) refers to the volume of Pb(II) ions solution; and $m$ (g) represents the mass of added fiber membrane. Additionally, $c_0$ ($mg \cdot L^{-1}$), $c_t$ ($mg \cdot L^{-1}$), and $c_e$ ($mg \cdot L^{-1}$) symbolize the concentrations of Pb(II) ions at the initial, $t$ (min), and after the adsorption equilibrium, respectively.

### Practical application

Pb(II) ions with various designed concentrations were introduced into bottled beverages, such as spring water, green tea drinks, and liquor (Baijiu in China), to investigate the adsorption capacity of the PVA/PAA/DMTD ENFM for removing Pb(II) ions in liquid food. Following microwave digestion, the residual solution concentrations of Pb(II) and other metal ions before and after reaching adsorption equilibrium were analyzed using ICP-MS. Upon the absorption of Pb( II) ions in green tea drinks, tea polyphenol (TPP) contents in the beverages were determined using a standard method established by the Chinese authorities.

## QUANTIFICATION AND STATISTICAL ANALYSIS

All experiments in the adsorption kinetics, isothermal and thermodynamic studies were repeated three times and averaged for model fitting. The coefficients of determination ($R^2$) were used to determine the fitting effect. All other experiments were repeated three times and data are represented as means ± SDs.